MODELLING AND SIMULATION OF BIFACIAL SOLAR PV SYSTEMS

A PROJECT REPORT

Submitted by

A. RAHUL ARAVIND [RA1711002010024]

PRASANTH CHOWDARY. Y [RA1711002010049]

Under the guidance of

Mr. JOJI JOHNSON

(Assistant Professor, Department of Mechanical Engineering)

In submission for assessment and award

Of grade

BACHELOR OF TECHNOLOGY

In

MECHANICAL ENGINEERING

FACULTY OF ENGINEERING AND TECHNOLOGY

S.R.M. Nagar, Kattankulathur, Kancheepuram District

MAY 2021

SRM UNIVERSITY

(Under Section 3 of UGC Act, 1956)

BONAFIDE CERTIFICATE

Certified that this project report titled "**Modelling and Testing of Bifacial solar PV systems**" is the bonafide work of "**A. RAHUL ARAVIND [Reg No: RA1711002010024], PRASANTH CHOWDARY. Y [Reg No: RA1711002010049]**" who carried out the project work under my supervision. Certified further, that to the best of my knowledge the work reported herein does not form any other project report or dissertation on the basis of which a degree or award was conferred on an earlier occasion on this or any other candidate.

SIGNATURE   SIGNATURE

MR. JOJI JOHNSON   Dr.M.CHERALATHAN

GUIDE   **HEAD OF THE DEPARTMENT**
Assistant Professor   Dept. of Mechanical Engineering
Dept. of Mechanical Engineering

Signature of the Internal Examiner   Signature of the Internal Examiner

ABSTRACT

Bifacial photovoltaic system produces solar power from both sides of the panel by absorbing sunlight from the sun directly and also by the means of reflected and diffused rays that fall on both the front and rear side of the panel. Bifacial solar modules can be installed both in vertical and horizontal orientation with each offering different benefits. Bifacial solar modules offer an interesting price/performance ratio. Much work has been focused on the tilt angle, orientation and directing the ground albedo to the panel. In this paper, we will test the panel by increasing the height in two different settings: 1 meter and 1.5 meter. By this we increase the overall efficiency of solar panel. We will see the optimal parameters and conditions for the most efficient installation and testing for the given location.

ACKNOWLEDGEMENT

TABLE OF CONTENTS

LIST OF FIGURES

LIST OF TABLES

LIST OF SYMBOLS

V_{mp} …………. Voltage at maximum power

V_{oc} ………...…. Voltage at open circuit

F.F ……………. Fill factor

I_{mp} ……………. Current at maximum power

I_{sc} ……………… Short circuit current

P_{mp} …………… Maximum power point

GHI …………… Global horizontal irradiance

DHI …………… Diffused horizontal irradiance

ρ_P ……………… Albedo of the ground

θ ………………. Incident angle

θ_Z ……………… Zenith angle

ω ……………... Hour angle

H_P ………….…… Height of the panel

E_P ………….……. Elevation of the panel

B_P ……………. Tilt angle

CHAPTER 1: INTRODUCTION

The bifacial solar cells were a recent innovation to the mainstream solar cell market by the early 2010. The bifacial solar panel is capable of producing direct current by absorbing the sunlight on both the sides of the panel. This is due to the availability of solar cells on either side which is separated by a layer of insulation in the centre. They over an interesting price to performance ratio as they are more efficient when considered to the mono-facial technology.

1.1 Factors Affecting the Efficiency

The production of energy from a bifacial panel depends on several factors for efficiency. The ground albedo, determines the amount of energy that the rear side absorbs. The tilt angle of the panel that it is set in affects the sunlight that falls directly on the surface of the cells. The height of the panel from the ground determines how much reflected light falls on the rear and some of front side. The module efficiency depends on other external factors like temperature, wind and other external factors.

1.2 About the Project

To increase the efficiency of the module, we will be testing the panel at different heights with respect to the surface, thus by increasing the height, we will study the increase in the efficiency due to the uniformity of the reflected light that falls on the module on the rear side. The height variation conducted in this experimental setup is considered at 1 meter and 1.5 meter.

1.3 Anatomy of Bifacial Module

The bifacial solar panel consists of PV module (cells on either sides of the panel) It has collector plates which conduct the heat falling on the cells and collecting pipes.
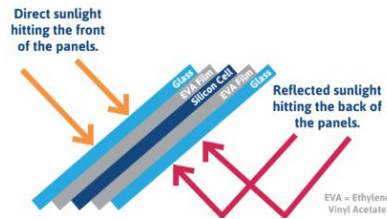
Figure 1: Anatomy of Bifacial Module

All these are separated by an insulation in the centre of the panel differentiating the sides to be front and rear.

1.4 Module Specifications

The bifacial panel has a maximum wattage of 195 watts, meaning the panel will be able to produce 195 watts of energy at a given time at given STC condition.

The maximum irradiance that falls on the panel surface is measured at 100 mW/cm^2.

Vmp is the voltage that will be available when the module is connected to a load and is working at a maximum operating capacity and under its STC conditions.

V_{oc} is the voltage across the panel that is measured when there is no load connected to the system. This is an important test as it suggests the number of modules required for a particular load capacity.

Table 1: Module Specifications

Module	195W
Irradiance (mW/cm²)	100
Vmp (V)	20.295
Voc (V)	24.3804
F.F	79.24
Model Area (cm²)	9875.25
Imp (A)	9.7611
Isc (A)	10.2541
Pmp (W)	198.1019
Module efficiency (%)	20.56

F.F is a factor that determines the maximum power of a solar module that is produced to the product of V_{oc} and I_{sc}.

Model are is the total area of the panel, which is of length 1485mm and breadth of 665mm.

I_{mp} is the current that is produced by the module when its operating at maximum power.

I_{sc} is the current value produced when the terminals of the panel are connected to each other to an ammeter in series. This is the maximum current that the module is capable of producing at the STC conditions.

P_{mp} is the maximum power the panel is able to produce at the standard conditions.

CHAPTER 2: LITERATURE REVIEW

2.1 Altitude and Elevation

Stanley Wang (2015) depicts that at lower altitude, higher elevation is required. A surface with high reflection coefficient yields a higher energy. Addition to this, there should be ample space available for the array modules as to achieve this high energy yield, there shouldn't be any obstruction. With the current setting, it was proved to achieve an increase in over 10% energy yield using a multi-crystalline cell with a bifaciality of 0.6 factor.

2.2 Albedo Factor and Reflectors

Muhammad Ashraful Alama (2018) provides a global study and enhancement of bifacial panels. Low ground albedo of 0.25 factor can give a gain of 10%. But by increasing the albedo factor using reflectors to 0.5 and increasing the height to 1 meter, the gain substantially increased to 30%. The vertical east-west facing installation in this configuration is more efficient than the south facing, as it reduces the self-shading.

2.3 Under Realistic Test Conditions

Ismail Shoukry (2016) discuss about the bankability of bifacial panels under realistic conditions as at the end of the day, cost per performance is the most important factor undermining the rest. In the software simulation, the panel was able to output at bifacial gain of 33%, but infield installation setup efficiency was ranging from 31.4% to 27.7%. The decrease was due external factors infield such as self-shading, wind and other factors.

2.4 Soiling and Cleaning

Rodrigo Escobar (2018) explains the importance of soiling and cleaning on a periodic basis. During an experimental period, dust storm caused the panel to lose efficiency until cleaned. The test was conducted for the ratio between circuit current and global radiance in a 60-day outdoor exposure before cleaning, the ratio was considered as 0% and after cleaning the ratio was -12.75% and for mono-facial it was -17.25%. In a year around the loss is calculated to be 21.6% lower than the full efficiency otherwise.

2.5 Efficient Methods to Increase Reflectivity

J. Frank (2012) conducted a test where they were able to analyze the performance of the bifacial panel with reflectors for the front and rear side and without the reflectors. They used samples such as white paint, paper, silver coated mirror and PTFE. These samples contained both textured and planar surface. The test results showed that the most efficient method was to use textured for the front and for the rear solar cells. This was because these irregularities were able to trap the light better and reflect.

2.6 Performance Assessment using Simulation Software

Katsaounis T (2019) emphasizes the efficacy of bifacial PV cells by findings their potential through simulations and modelling experiments. The simulation is conducted solely for the transport equation solutions and outdoor experiment for getting applied results. Mono-facial panels were used for comparative study. The numerical values were attained through linear finite element analysis and the input was obtained from outdoor environmental parameters. The simulation and experiment were compared based on the current-voltage values calculated in respective methods.

2.7 Yield Prediction using Miniaturised System

Nussbaumer H (2019) says the corresponding paper compares the energy output of a small-scale bifacial PV system with that of a commercial bifacial system. The commercial bifacial PV system is set up as a 3 x 3 array of 60-cell modules namely Megacell MBF-GG60-270 and the array is termed BIFOROT (Bifacial Outdoor Rotor Tester). The miniature version is of the same cell setup with a scale of 1:12, which was chosen for quick mounting and testing purposes. The results were compared with respect to the daily scaling factor and the reading were taken for various tilt angles. Plots were made nominal power at different timings at a particular tilt angle. The main aim was to conclude if a miniaturized version of a bifacial PV system is viable for testing to make optimisation parameters an easy calculation.

2.8 Effect of Temperature on the system

Patel M. T (2020) explains the effect of temperature-dependent efficiency on the energy yield and levelized cost of energy is studied in this paper. Factors such as input irradiance, environmental conditions, mounting configurations, type of cells and module setup, thermal coefficient are taken into consideration to divulge the efficiency characteristics. The experiment is done on both mono-facial and bifacial PV modules for comparative purposes and between single bifacial PV module and a bifacial farm to check the efficiency and energy degradation trends. The results are compared with that of existing physically validated temperature-dependent efficiency models across the world.

2.9 Energy Yield due to Shading

Zhu Q (2019) Explains the shading effect on the modules due to the panel area and additional accessories such as wires, frames and holders is discussed in this paper. Height of the panel is from the ground is also subjected to change due to considerable effect on shading phenomenon. An optical model for both wires and frame is created to check the optical loss and compared with the experimental results where frames and wires are kept a varied height from the ground to see their effect on shading, Isotropic light is used for negligible deviation due to shading and the results are plotted on graph showing the optical loss variation with the height changes. The shading effect or optical loss is given by fraction between shading angle and 90°.

2.10 Energy Yield in Simulation

Chudinzow D (2019) reviews the current energy yield model and proposes improvement techniques. Simulation of a bifacial power plant is done using tools such as NREL's SAM, PVsyst, MoBiDiG and BIGEYE for accounting various parameters like view factors, irradiation from all source points, LCOE, shading effect etc. The modelling is divided into input, calculation and result and written using MATLAB. The Chilean bifacial PV power plant, La Hormiga in San Felipe was taken as reference for this model. The plant was downscaled to a capacity of 19.44kWp for simulation. Upon getting results, improvement on ground reflectivity, shading area, tilt angles were provided.

2.11 Reducing Transmittance losses

Yong Sheng Khoo (2017) conducted several techniques to reduce transmittance losses and increase its performance. For the rear panel, they coat it with infrared reflective coating which allows a gain up to 1%. Further it is coated with white on the cell-gap area for glass/glass panel, where gains up to 3% is noticed. They have also demonstrated that by texturing the panel the efficiency can be further increased. Hence doing so, they were able to increase the overall gain by 4% for the glass/glass panel and decreasing the cost/watt.

2.12 Test under Real World Conditions

Xiaochun Zhang and Tao Ma (2020) investigated the performance of bifacial panel in real world conditions with taking mono-facial panel as reference. The parameters that affect the power output, irradiance distribution and energy yield are ground albedo, tilt angle and orientation. With ground albedo, the different surfaces were used like aluminium and grass. Aluminium gave more output due to higher albedo value. Tilt angle at 30° produces more due to higher irradiance. The south facing orientation produces the most output due to the higher irradiance.

2.13 Effect of Albedo on Bifacial Panels

The paper discusses the effect of albedo on the back of a bifacial photovoltaic cell and compares the efficiency of the panel with that of a monofacial under similar conditions (STC-AM 1.5G; 1 sun; 100mW/cm2) and the results provided in Jsc (mA/cm2). Bifaciality factor is used to compare the performance of both sides and modelling of the panel is also done under same circumstances as listed above using SunSolveTM . The calculations are done in the same software with comparisons of both the panels under varying albedos are provided.

CHAPTER 3: SYSTEM ANALYSIS

3.1 Mathematical Model Calculation

3.1.1 Calculating the irradiance for the front side of the module

Equation 1: Front irradiance

$$G_F = G_b^F + G_d^F + G_r^F = (GHI - DHI) \cdot R_b^F + DHI \cdot X_{F-sky} + GHI \cdot X_{F-grd}$$

Equation 2: Ratio of tilted irradiance and horizontal irradiance

$$R_b^F = \begin{cases} \dfrac{cos\emptyset^F}{cos\emptyset_Z^F}, & \gamma_P - \dfrac{\pi}{2} \leq \omega \leq \gamma_P + \dfrac{\pi}{2} \\ 0, & \omega < \gamma_P - \dfrac{\pi}{2} \, or \, \omega > \gamma_P + \dfrac{\pi}{2} \end{cases}$$

Equation 3: View factor for front side

$$\text{From panel to sky: } X_{F-sky} = \frac{1+cos\beta_p}{2}$$

$$\text{From panel to ground: } X_{F-grd} = \frac{1-cos\beta_p}{2}$$

Schematic Diagram of the panel and its values
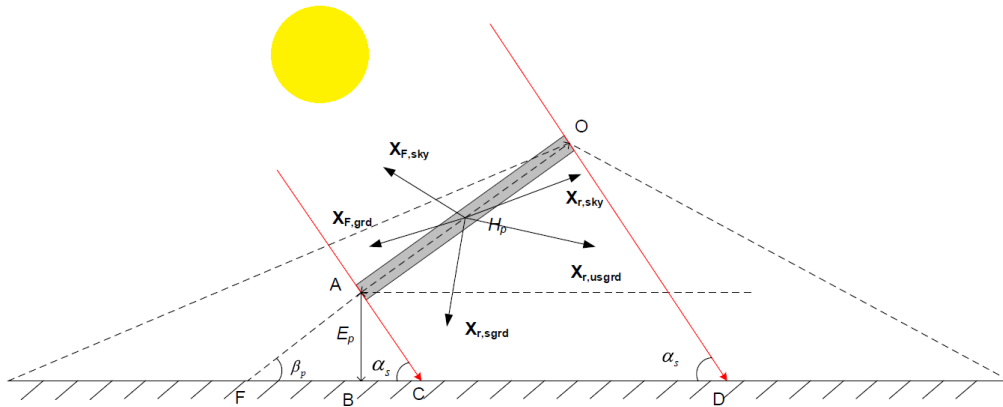
Figure 2: Schematic diagram for panel and its angles

3.1.2 Calculating the irradiance for the rear side of the module

Equation 4: Rear irradiance

$$G_F = G_b^R + G_d^R + G_r^R$$

$$= (GHI - DHI) \cdot R_b^R + DHI \cdot X_{R-sky} + GHI \cdot \rho_P \cdot X_{R-usgrd} + DHI$$

$$\cdot GHI \cdot \rho_P \cdot X_{R-sgrd}$$

Equation 5: Ratio of rear tilted and horizontal irradiance

$$R_b^R = \begin{cases} 0, & \gamma_P - \dfrac{\pi}{2} \leq \omega \leq \gamma_P + \dfrac{\pi}{2} \\ \dfrac{cos\emptyset^F}{cos\emptyset_Z^F}, & \omega < \gamma_P - \dfrac{\pi}{2} \; or \; \omega > \gamma_P + \dfrac{\pi}{2} \end{cases}$$

Equation 6: View factors for rear side

From panel to sky: $X_{R-sky} = \dfrac{1-cos\beta_p}{2}$

Rear side to the unshaded ground:

$$X_{R-usgrd} = X_{R-DQ} + X_{R-CF}$$

$$X_{R-DQ} = \frac{X_{OF-DQ}^R \cdot \overline{OF} - X_{AF-DQ}^R \cdot \overline{AF}}{\overline{OA}}$$

$$X_{R-CF} = \frac{X_{OF-CF}^R \cdot \overline{OF} - X_{AF-CF}^R \cdot \overline{AF}}{\overline{OA}}$$

$$X_{OF-DQ}^R = X_{OF-FQ}^R - X_{OF-FD}^R = \frac{1 + cos\beta_p}{2} - \frac{\overline{OF} + \overline{FD} - \overline{OD}}{2\overline{OF}}$$

$$X_{AF-DQ}^R = X_{AF-FQ}^R - X_{AF-FD}^R = \frac{1 + cos\beta_p}{2} - \frac{\overline{AF} + \overline{FD} - \overline{AD}}{2\overline{AF}}$$

$$X_{OF-CF}^R = \frac{\overline{OF} + \overline{CF} - \overline{OC}}{2\overline{OF}}$$

$$X_{AF-CF}^R = \frac{\overline{AF} + \overline{CF} - \overline{AC}}{2\overline{AF}}$$

$$\overline{OA} = H_P; \quad \overline{OF} = \sqrt{(H_P \cos\beta_p + \frac{E_P}{\tan\beta_P})^2 + \sqrt{(E_P + H_P \sin\beta_P)^2}}$$

$$AF = \frac{E_P}{\sin\beta_P}; \quad \overline{OD} = \sqrt{(H_P \cos\beta_P - \frac{E_P \cos\alpha_S + H_P \sin(\alpha_S + \beta_P)^2 + (E_P + H_P \sin\beta_P)^2}{\sin\alpha_S}}$$

$$AC = \frac{E_P}{\sin\alpha_S}; \quad \overline{CF} = E_P\left(\frac{1}{\tan\alpha_S} + \frac{1}{\tan\beta_P}\right); \quad \overline{FD} = \frac{H_P}{\sin\alpha_S}\sin(\alpha_S + \beta_P) + \frac{H_P}{\tan\beta_P} + \frac{H_P}{\tan\alpha_S};$$

$$\overline{OC} = \sqrt{(H_P \cos\beta_p - \frac{E_P}{\tan\alpha_S})^2 + (E_P + H_P \sin\beta_P)^2}$$

$$\overline{AD} = \sqrt{\left(\frac{E_P \cos\alpha_S + H_P \sin(\alpha_S + \beta_P)}{\sin\alpha_S}\right)^2 + E_P{}^2}$$

Rear side to the shaded ground: $X_{R-sgrd} = \frac{\overline{OC} + \overline{AD} - (\overline{AC} + \overline{OD})}{2\overline{OA}}$

3.2 GHI and DHI Values from PVsyst

Values for global horizontal irradiance (GHI) and diffused horizontal irradiance (DHI) were taken using the PVsyst software
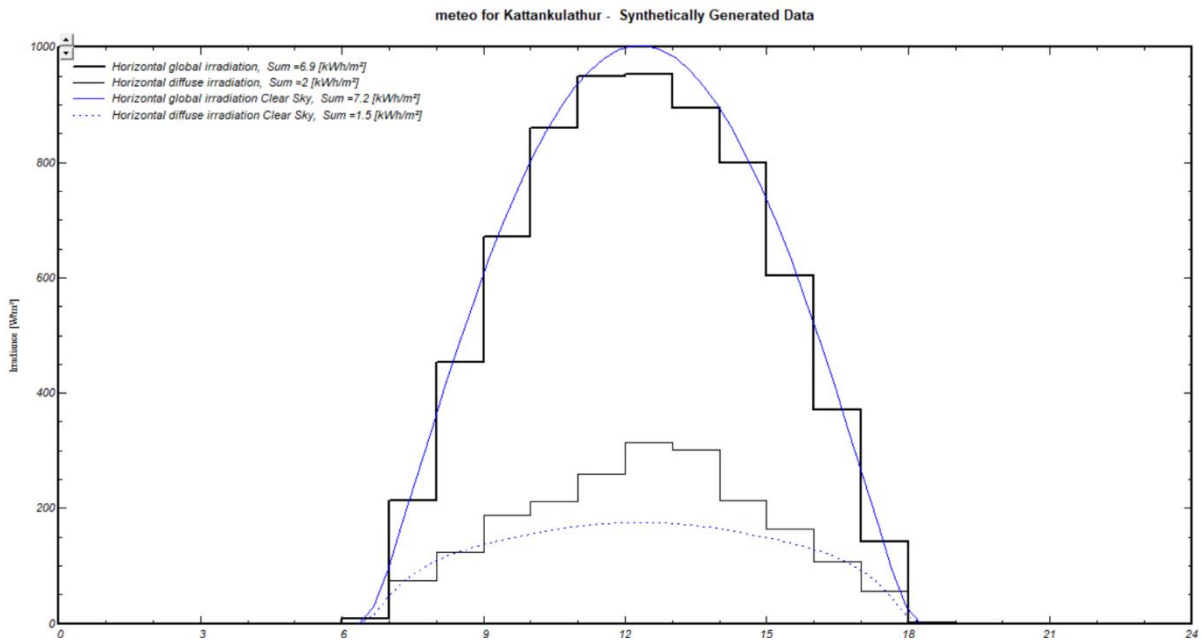
Figure 3: GHI and DHI graph

The required values for the mathematical calculation were taken at an interval of 2 hours at 8AM, 10AM, 12PM, 2PM, 4PM.

Table 2: GHI& DHI Values

TIME	DHI	GHI
8AM	74kW/m²	215kW/m²
10AM	190kW/m²	680kW/m²
12PM	260kW/m²	940kW/m²
2PM	215kW/m²	900kW/m²
4PM	110kW/m²	600kW/m²

3.3 Results and Graphs from Mathematical Model

From Table 3 we can see the results for the irradiance for front side, rear side for both 1 meter and 1.5 meters that were found using the following equations given above. The front side irradiance will remain the same or have negligible increase with increase in height. But when it comes to the rear side, the increase in 0.5 meters will increase the output in a significant rate. This is because of the increase in albedo noticed as the height increases. The spread of the reflected rays increases and reaches rear side of the panel much more efficiently.

Table 3: Irradiance Result from calculation

TIME	G_F Front side Global irradiance(W/m²)	$G_{R \ (1 \ METER)}$ Rear side Global irradiance(W/m²)	$G_{R \ (1.5 \ METER)}$ Rear side Global irradiance(W/m²)
		(1 meter height)	(1.5 meter height)
8:00 AM	190.1	81.463	165.908
10:00 AM	1035	290.035	311.93
12:00 PM	1383	402.34	435.36
2:00 PM	753.1	322.55	342.68
4:00 PM	234.6	207.12	271.29

Global irradiance for front and rear side (1 meter)

The increase in irradiance (W/m^2) in total is observed to be 223.66 W/m^2 for the 5 hours alone. Hence, we can say that the increase throughout the day will be significant. And when we see it on a long term, a year or more than a year, the increase in output will be large
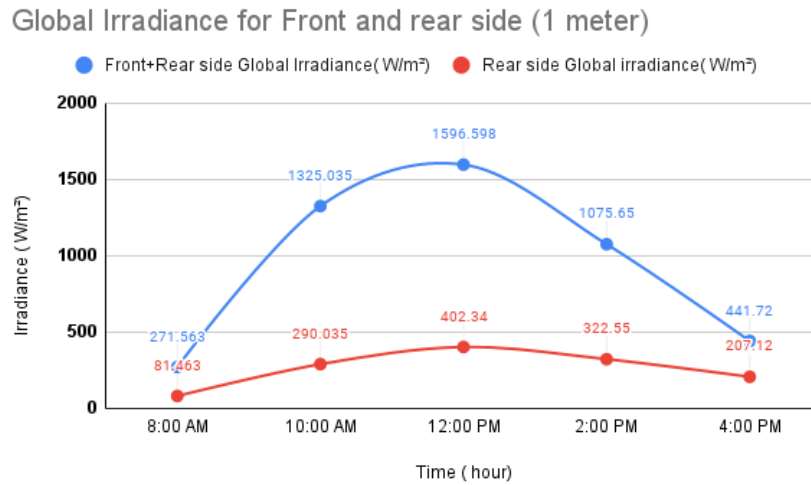
Figure 4: Global Irradiance (1 meter)

Global irradiance for front and rear side (1.5 meter)
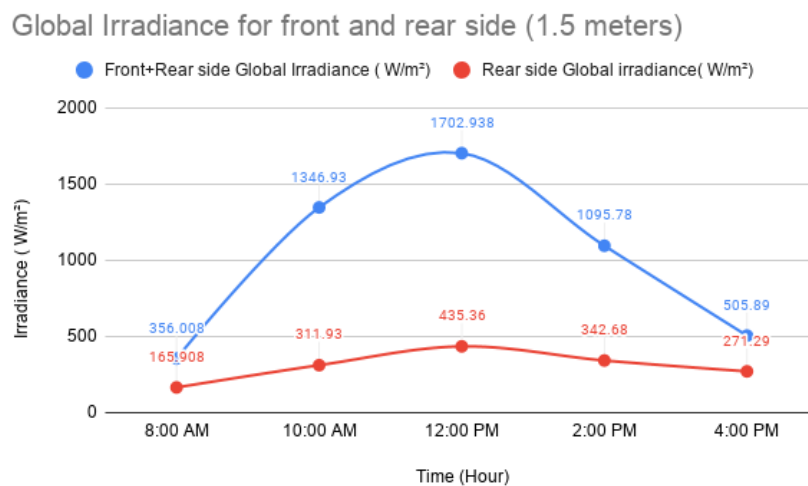
Figure 5: Global Irradiance (1.5 meter)

3.3.1 Difference in Ground Albedo

The spread in albedo is visualized on the Figure 6, it shows the increase in spread of albedo from ground back towards the module. The further the panel gets, more the albedo hits the rear side of module.
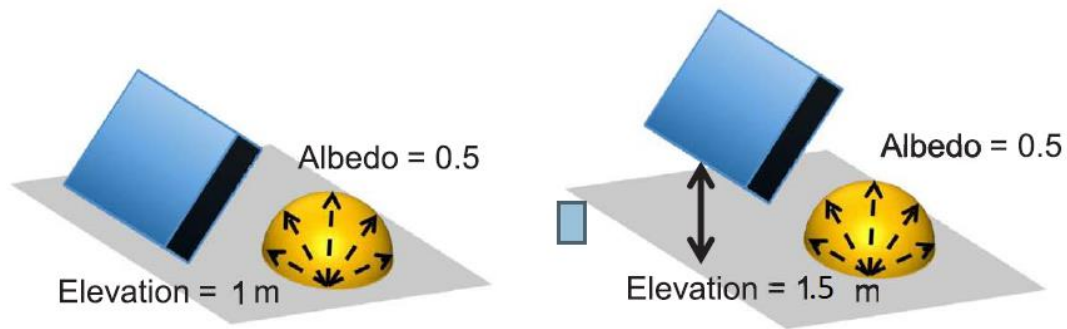
Figure 6: Difference in albedo spread due to increase in height

3.3.2 Difference in rear irradiance

The difference in the rear irradiance is show for 1 meter and 1.5 meters in Figure 4 and Figure 5 respectively. In Figure 7 we can the increase peaks and lows for the rear irradiance. At 8AM and at 1PM the increase in rear side is significant. So, we capitalise on this as well, as we increase the number of peaks gained by the module.
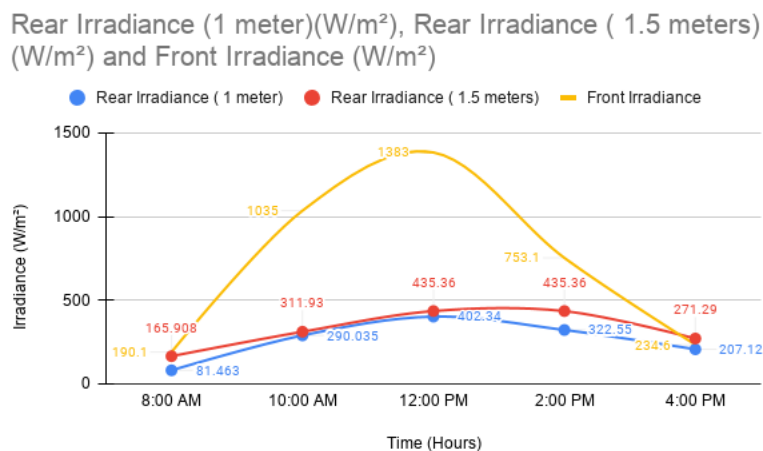
Figure 7: Increase in rear irradiance (1 meter vs 1.5 meter)

3.3.3 Hour angle versus Time graph

From Figure 8 we can see the different hour angles of the sun as it changes its angular angle each hour with respect to the module. Using this we get the best peak for the module.
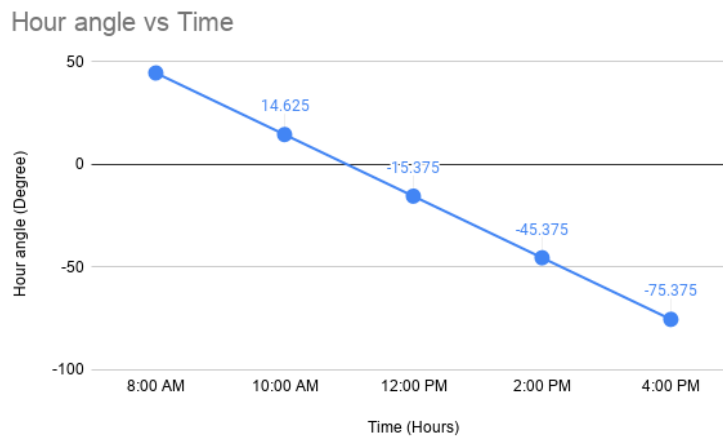
Figure 8: Hour angle vs Time

3.3.4 Angle of Incidence vs Time graph

The angle of incidence shows the angle at which the irradiation from the sun comes in contact with the module face. This has a U-curve.
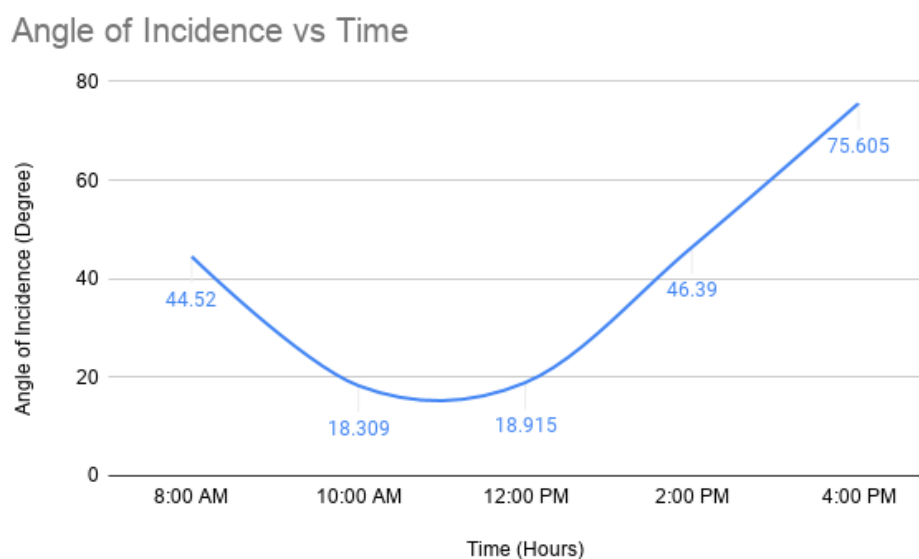
Figure 9: Angle of incidence vs time

3.4 Project Setup

3.4.1 Bifacial Solar Panel

Front side, backside, cell close up respectively
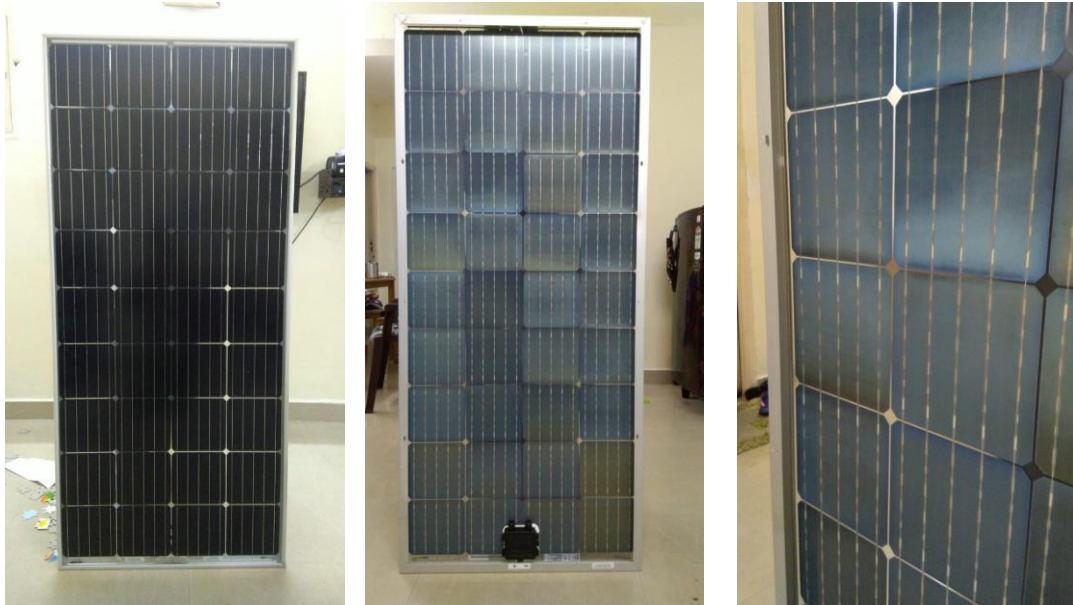
Figure 10: Front side, Rear and Close up of cell

3.4.2 Instruments Required for measurement

DC Voltmeter. Rating up to 50V. It has an accuracy class of 0.5 (0.5% of range) It has an insulation force of 50KV at 50Hz.

Figure 11: Voltmeter

DC Ammeter. Rating up to 50A. The ammeter is considered after the maximum amperage the module can pass. The operating temperature range is of 20°C-50°C, has an accuracy class of 1 (1% of range).

Figure 12: Ammeter

Resistor with a rating of 2 ohms. The resistor is found for the following system as per the Ohms law.

Figure 13: Resistor

3.4.3 Support Structure
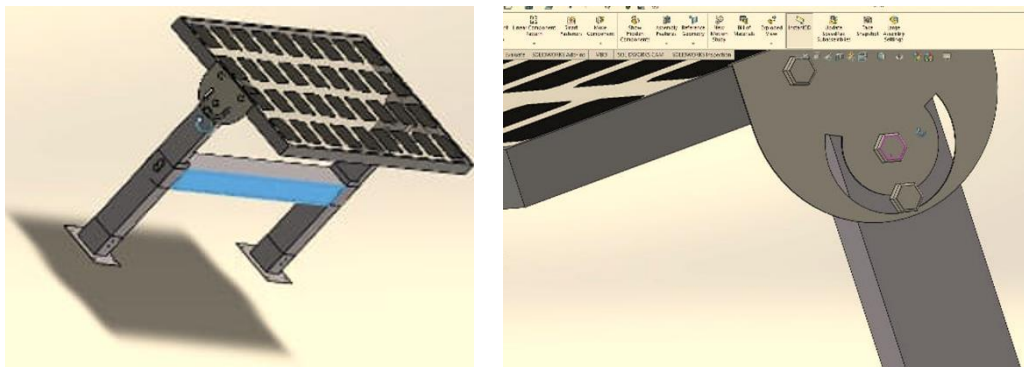
Figure 14: Support structure with angle adjustment

3.4.4 Project Layout

The circuit is connected as shown. The ammeter is connected in series with the load and the negative of PV panel. The voltmeter is connected in parallel with the load and negative of the panel. Thus, they show the values of the same.
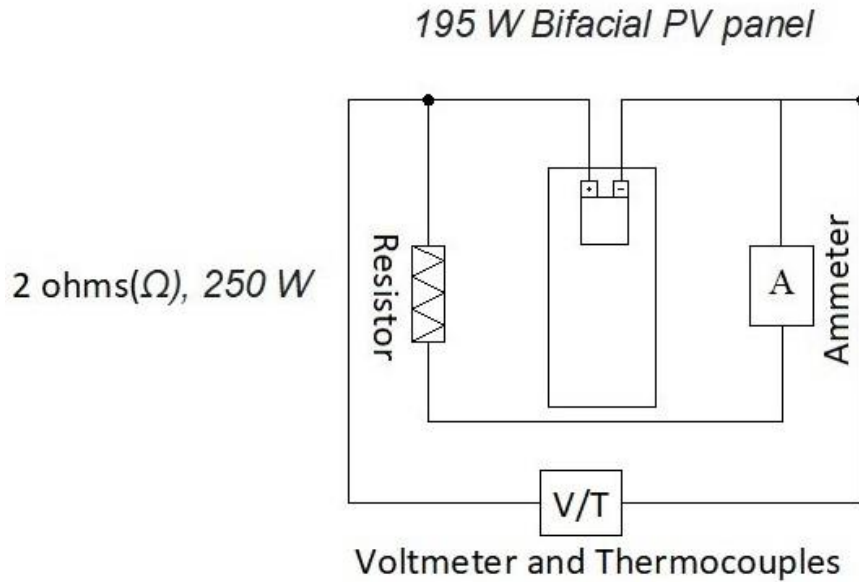
Figure 15: Setup Layout

In diagram Figure 9 the bifacial panel procured for the project this project is shown having the dimensions of (1485 x 665 x 2.2) mm. With having module area of 9875.25mm^2. It has a setup of 36 cells in series and 1 parallel. Each cell area of just over 275 mm^2 of cell area. The panel weights 11.6 kilograms.

The measuring instruments are a voltmeter, ammeter and a resistor. The voltmeter is considered after the maximum voltage of the module. The resistor is found using the formula

Equation 7: Resistance calculation

$$R = \frac{V}{I} = \frac{20.295}{9.7611} = 2.097 \: Ohms$$

The resistor used will be of 2Ω and 200W, from the following data.

The support structure was done using AutoCAD software and constructed as per the panel dimensions and have the feature which allows an increase in height by adjusting the leg spokes and to extend them. It also has an angle adjustment instrument which consists of a plate and bolts which lock the panel at the required angle by tightening the bolts. The structure spans over a length of 1485mm and has an angle adjustment of every 15° starting from 0°. The stand legs can be increased from a minimum height of 1 meter to the maximum height of 1.5 meters.

The setup layout is done by connecting the module's positive with a resistor and load the negative with ammeter and load. The ammeter is connected in series, when the load consumes the power, the reading in ammeter is shown. The voltmeter is connected in parallel as it finds the potential difference between the two points and tells the voltage across the setup.

In the setup, the voltmeter is connected with a thermocouple that is used to find the temperature of the panel and to regulate it. It gives a real-time temperature output for the setup.

CHAPTER 4: SIMULATION

4.1 Simulation using PVsyst (Before Consumption)

A grid based solar system for a 2.5kW system. The following appliances were considered.

APPLIANCE	WATTAGE (w)	UNITS	TOTAL WATTAGE (w)
TUBELIGHT	50	5	250
FAN	75	5	375
FRIDGE	1000	1	1000
TV	175	1	175
DESKTOP	450	1	450
MISC	250	1	250
			2500

Table 4: Appliance Power Rating

The above-mentioned appliances were considered for their common usage in most households. The wattage and the number of units were taken as of standard values to depict a 2.5kW system to be supported by grid based solar system.

4.1.1 Location and System Summary

The geographical location was considered to be the site of Main campus in SRM Institute of science and technology, Kattankulatur.

Project summary

Geographical Site	Situation		Project settings	
Kattankulathur	Latitude	12.82 °N	Albedo	0.20
India	Longitude	80.04 °E		
	Altitude	43 m		
	Time zone	UTC+5.5		

Meteo data
Kattankulathur
Meteonorm 8.0 (1996-2015) - Synthetic

System summary

Grid-Connected System	Unlimited sheds			
PV Field Orientation	**Near Shadings**		**User's needs**	
Sheds	Mutual shadings of sheds		Unlimited load (grid)	
tilt	15 °	Electrical effect		
azimuth	0 °			
System information				
PV Array		**Inverters**		
Nb. of modules	13 units	Nb. of units		1 Unit
Pnom total	2535 Wp	Pnom total		2500 W
		Pnom ratio		1.014

The specified coordinates of 12.82 °N Latitude and 80.04 °E is the specific location of the mechanical block in main campus.

The necessary specifications of the solar panel was given as input. The simulation resulted in amounting the panel units to 13 giving a nominal power of 2535 Wp, a little above the required 2.5kW. An inverter is also accounted to convert the variable DC output of the PV panel into a utility frequency alternating current (AC) that can be fed to the electrical grid.

4.1.2 General Parameters

The general parameters include the specifications or values used to setup the solar panel system on for power generation. The Angle of tilt is taken as 15° which is considered optimum for the given location and its coordinates. Since the panels are facing in the southern direction, the azimuth angle is taken as 0° since it is shows the direction of the sunlight coming in the view of a compass.

General parameters

Grid-Connected System   **Unlimited sheds**

PV Field Orientation

Orientation		Sheds configuration		Models used	
Sheds		Nb. of sheds	44 units	Transposition	Perez
tilt	15 °	Unlimited sheds		Diffuse	Perez, Meteonorm
azimuth	0 °	**Sizes**		Circumsolar	separate
		Sheds spacing	6.00 m		
		Collector width	2.00 m		
		Ground Cov. Ratio (GCR)	33.3 %		
		Top inactive band	0.02 m		
		Bottom inactive band	0.02 m		
		Shading limit angle			
		Limit profile angle	7.4 °		
		Shadings electrical effect			
		Cell size	15.6 cm		
		Strings in width	3 units		

Horizon		**Near Shadings**		**User's needs**	
Free Horizon		Mutual shadings of sheds		Unlimited load (grid)	
		Electrical effect			

Bifacial system					
Model	2D Calculation				
	unlimited sheds				
Bifacial model geometry				**Bifacial model definitions**	
Sheds spacing	6.00 m			Ground albedo	0.50
Sheds width	2.04 m			Bifaciality factor	80 %
Limit profile angle	7.5 °			Rear shading factor	5.0 %
GCR	34.0 %			Rear mismatch loss	10.0 %
Height above ground	1.50 m			Module transparency	0.0 %

The simulation uses Perez transposition model used in the calculation of the incident irradiance on tilted planes from horizontal irradiance data.

The sheds on which the system of solar panels were to be placed was taken as 44 units with a spacing of 6m. Ground cover ratio is shown to 33.33% which tells the ratio of the module area to the entire area of the system area.

In other words, the area of the array used for conversion of the sunlight captured. The limit shading angle that produces shade on to subsequent sheds was taken as 7.4 °. The simulation was conducted for both heights of 1 m and 1.5m with the albedo to be taken as 0.5.

4.1.3 Detailed Losses

Soiling losses are the losses incurred due to the accumulation of dirt, dust, leaves and other particles that get deposited on top of the panels or anywhere in the array that can affect the ground albedo.

Soiling losses of various months shows how seasons affect the power produced by a solar panel. During winter and rainy seasons, due to heavy winds and precipitation, incur more losses than in summer seasons which include less winds and rains. Other losses such as thermal loss, wiring loss due to resistance, quality loss over time is also included.

Array losses

Array Soiling Losses
Average loss Fraction   2.7 %

Jan.	Feb.	Mar.	Apr.	May	June	July	Aug.	Sep.	Oct.	Nov.	Dec.
3.0%	3.0%	3.0%	3.0%	3.0%	1.0%	1.0%	3.0%	3.0%	3.0%	3.0%	3.0%

Thermal Loss factor
Module temperature according to irradiance
Uc (const)   29.0 W/m²K
Uv (wind)   0.0 W/m²K/m/s

DC wiring losses
Global array res.   136 mΩ
Loss Fraction   0.5 % at STC

LID - Light Induced Degradation
Loss Fraction   2.5 %

Module Quality Loss
Loss Fraction   -0.5 %

Module mismatch losses
Loss Fraction   1.5 % at MPP

Strings Mismatch loss
Loss Fraction   0.1 %

IAM loss factor
Incidence effect (IAM): Fresnel AR coating, n(glass)=1.526, n(AR)=1.290

0°	30°	50°	60°	70°	75°	80°	85°	90°
1.000	0.999	0.987	0.962	0.892	0.816	0.681	0.440	0.000

System losses

Unavailability of the system
Time fraction   0.8 %
    2.7 days,
    3 periods

AC wiring losses

Inv. output line up to injection point
Inverter voltage   208 Vac mono
Loss Fraction   1.1 % at STC
Inverter: PVI 2500-208
Wire section (1 Inv.)   Copper 1 x 2 x 3 mm²
Wires length   14 m

4.1.4 Loss Diagram

Soiling losses are the losses incurred due to the accumulation of dirt, dust, leaves and other particles that get deposited on top of the panels or anywhere in the array that can affect the ground albedo.

Loss diagram

1856 kWh/m²	**Global horizontal irradiation**
+1.7%	**Global incident in coll. plane**
-0.57%	Near Shadings: irradiance loss
-2.17%	IAM factor on global
-2.69%	Soiling loss factor
+0.22%	Ground reflection on front side

Bifacial

Global incident on ground
1212 kWh/m² on 44 m²

-50.00% (0.50 Gnd. albedo)
Ground reflection loss

-73.01% View Factor for rear side
Irrad. scale. 1:2

+0.76%	Sky diffuse on the rear side
0.00%	Beam effective on the rear side
-5.00%	Shadings loss on rear side
25.72%	**Global Irradiance on rear side (461 kWh/m²)**

1791 kWh/m² * 15 m² coll.   **Effective irradiation on collectors**

Figure 16: Loss diagram for sun irradiance (before consumption)

Soiling losses of various months shows how seasons affect the power produced by a solar panel. During winter and rainy seasons, due to heavy winds and precipitation, incur more losses than in summer seasons which include less winds and rains. Other losses such as thermal loss, wiring loss due to resistance, quality loss over time is also included.

Light induced degradation accounts to 2.5% of the losses which is the loss resulting from the performance degradation in the very first hours of exposition to sunlight in crystalline modules. Incidence angle modifier (IAM) loss factor gives the decrease in irradiance due to deflection from the actual angle of irradiance.

efficiency at STC = 17.04%	PV conversion, Bifaciality factor = 0.80
5563 kWh	**Array nominal energy (at STC effic.)**
-0.59%	PV loss due to irradiance level
-8.34%	PV loss due to temperature
0.00%	Shadings: Electrical Loss , sheds3 strings in width
+0.50%	Module quality loss
-2.50%	LID - Light induced degradation
-1.60%	Mismatch loss, modules and strings
-2.13%	Mismatch for back irradiance
-0.39%	Ohmic wiring loss
4764 kWh	**Array virtual energy at MPP**
-7.10%	Inverter Loss during operation (efficiency)
0.00%	Inverter Loss over nominal inv. power
0.00%	Inverter Loss due to max. input current
0.00%	Inverter Loss over nominal inv. voltage
-0.01%	Inverter Loss due to power threshold
0.00%	Inverter Loss due to voltage threshold
4426 kWh	**Available Energy at Inverter Output**
-0.69%	AC ohmic loss
-0.90%	System unavailability
4356 kWh	**Energy injected into grid**

Figure 17: Loss diagram for panel output (before consumption)

Unavailability of the system is when the solar panel does not work due to technical difficulties or other environmental factors and it is taken to be 2.7 days per year. AC wiring losses are also taken into consideration and mostly depends on the wire characteristics.

The various losses are divided onto the losses due to irradiance of the sun and losses incurred by panel. In Figure 15. We can see that the power decreases from 1856 kWh/m2 to 1791 kWh/m2 due to the losses such as soling loss, shading factor, IAM factor and albedo fraction and other view factors.

Few losses include to the power generated such as the ground reflection onto the front side of the panel which are very minimal to the power produced. Figure16. Shows the decrease from 5563 kWh to 4356 kWh due to thermal losses, LID factor, wiring loss and unavailability of the system which were already mentioned above.

4.1.5 Simulation Result and Graphs

The Table 5 shows the amount of energy that is generated by the whole system in an year with consdering all the losses and other factors of the year. This production rate is the final rate that the user will get.

GlobHor is the global horizontal energy that is avaiable to the system at that particular month of the year. DiffHor is the diffused horizontal energy which is available to the system at the same period of time. T_Amb is the temperature of the system surroundings.

EArray is the energy produced by the array of panels before it is sent to the invertor for the use by the household. The E_Grid is the energy that the system injects into the grid. This includes the losses from the invertor and other transmission losses. This will be the final energy that will be available to the user

Table 5: Main Results (Before consumption)

Main results

System Production

Produced Energy	4356 kWh/year
Specific production	1718 kWh/kWp/year
Performance Ratio PR	91.04 %

Normalized productions (per installed kWp)

Lc: Collection Loss (PV-array losses) 0.02 kWh/kWp/day
Ls: System Loss (inverter, ...) 0.44 kWh/kWp/day
Yf: produced useful energy (inverter output) 4.71 kWh/kWp/day

Performance Ratio PR

PR: Performance Ratio (Yf / Yr) : 0.910

Balances and main results

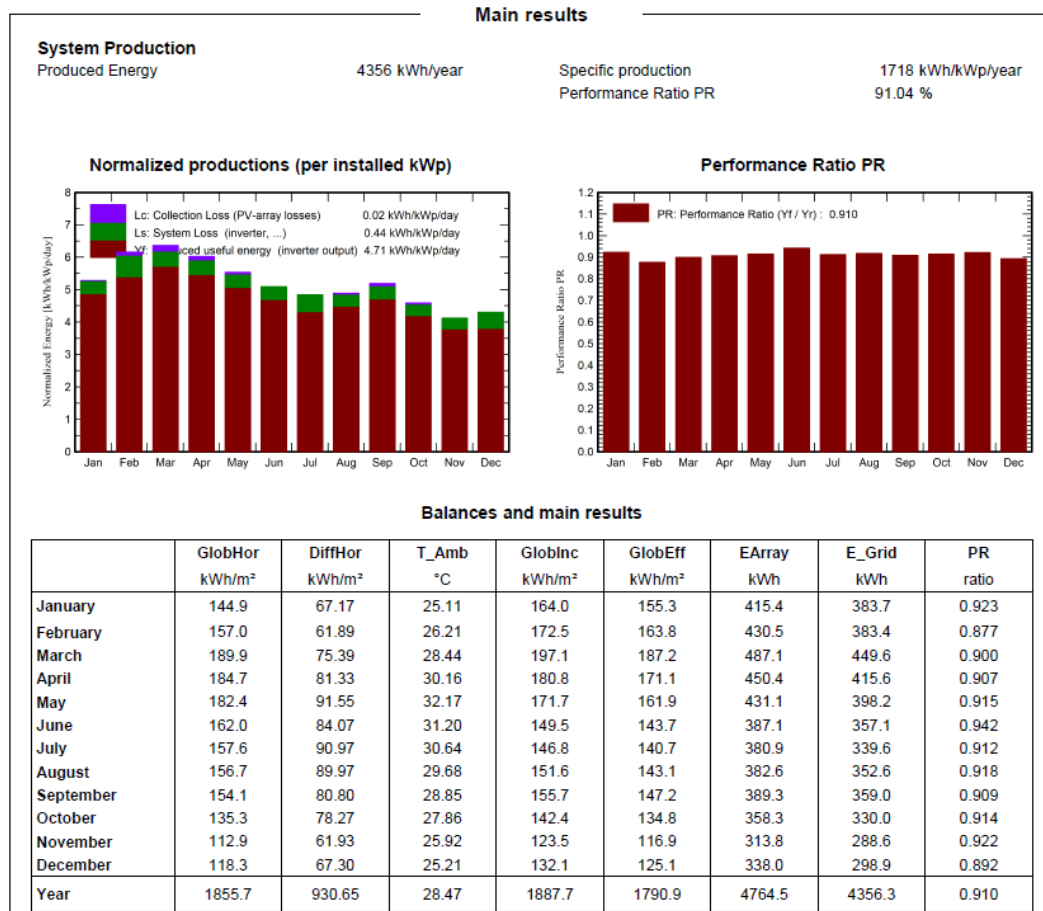|	GlobHor	DiffHor	T_Amb	GlobInc	GlobEff	EArray	E_Grid	PR
	kWh/m²	kWh/m²	°C	kWh/m²	kWh/m²	kWh	kWh	ratio
January	144.9	67.17	25.11	164.0	155.3	415.4	383.7	0.923
February	157.0	61.89	26.21	172.5	163.8	430.5	383.4	0.877
March	189.9	75.39	28.44	197.1	187.2	487.1	449.6	0.900
April	184.7	81.33	30.16	180.8	171.1	450.4	415.6	0.907
May	182.4	91.55	32.17	171.7	161.9	431.1	398.2	0.915
June	162.0	84.07	31.20	149.5	143.7	387.1	357.1	0.942
July	157.6	90.97	30.64	146.8	140.7	380.9	339.6	0.912
August	156.7	89.97	29.68	151.6	143.1	382.6	352.6	0.918
September	154.1	80.80	28.85	155.7	147.2	389.3	359.0	0.909
October	135.3	78.27	27.86	142.4	134.8	358.3	330.0	0.914
November	112.9	61.93	25.92	123.5	116.9	313.8	288.6	0.922
December	118.3	67.30	25.21	132.1	125.1	338.0	298.9	0.892
Year	1855.7	930.65	28.47	1887.7	1790.9	4764.5	4356.3	0.910

Figure 18: Main results (Before consumption)

23

Energy produced at monthly hourly average

Table 6 shows the amount of energy produced in an average hour of the day throought the year. The hours 10AM to 1PM are considered as peaks in this because they average the highest energy produciton in a day.

Table 6: Energy Produced at monthly hourly average

FINAL PROJECT 10/5
Monthly Hourly averages for E_Grid [kW]

	0H	1H	2H	3H	4H	5H	6H	7H	8H	9H	10H	11H	12H	13H	14H	15H	16H	17H	18H
January	0.00	0.00	0.00	0.00	0.00	0.00	0.00	0.32	0.83	1.24	1.53	1.68	1.71	1.65	1.46	1.15	0.69	0.11	0.00
February	0.00	0.00	0.00	0.00	0.00	0.00	0.00	0.33	0.87	1.36	1.68	1.86	1.88	1.80	1.60	1.27	0.80	0.25	0.00
March	0.00	0.00	0.00	0.00	0.00	0.00	0.00	0.45	1.03	1.51	1.88	1.93	1.93	1.90	1.64	1.24	0.76	0.24	0.00
April	0.00	0.00	0.00	0.00	0.00	0.00	0.06	0.57	1.09	1.51	1.79	1.77	1.81	1.73	1.49	1.15	0.68	0.20	0.00
May	0.00	0.00	0.00	0.00	0.00	0.00	0.13	0.56	1.01	1.37	1.63	1.69	1.70	1.58	1.35	1.04	0.60	0.18	0.00
June	0.00	0.00	0.00	0.00	0.00	0.00	0.11	0.49	0.94	1.28	1.52	1.53	1.55	1.46	1.28	0.95	0.59	0.20	0.00
July	0.00	0.00	0.00	0.00	0.00	0.00	0.07	0.41	0.82	1.13	1.37	1.40	1.44	1.38	1.19	0.92	0.59	0.22	0.00
August	0.00	0.00	0.00	0.00	0.00	0.00	0.03	0.42	0.84	1.18	1.47	1.51	1.53	1.48	1.23	0.93	0.57	0.19	0.00
September	0.00	0.00	0.00	0.00	0.00	0.00	0.03	0.51	0.99	1.28	1.51	1.54	1.51	1.49	1.34	1.05	0.57	0.13	0.00
October	0.00	0.00	0.00	0.00	0.00	0.00	0.02	0.45	0.89	1.18	1.38	1.51	1.43	1.32	1.20	0.84	0.41	0.01	0.00
November	0.00	0.00	0.00	0.00	0.00	0.00	0.01	0.36	0.71	1.03	1.24	1.34	1.40	1.30	1.09	0.79	0.36	0.00	0.00
December	0.00	0.00	0.00	0.00	0.00	0.00	0.00	0.30	0.61	0.98	1.17	1.32	1.43	1.38	1.23	0.83	0.40	0.00	0.00
Year	0.00	0.00	0.00	0.00	0.00	0.00	0.04	0.43	0.88	1.25	1.51	1.59	1.61	1.54	1.34	1.01	0.58	0.14	0.00

Normalized energy production

Graphs Figure 18 and Figure 19 gives a clear view on how the energy produced varies for different months of the year and the losses vary according to the seasonal variations that we experience.
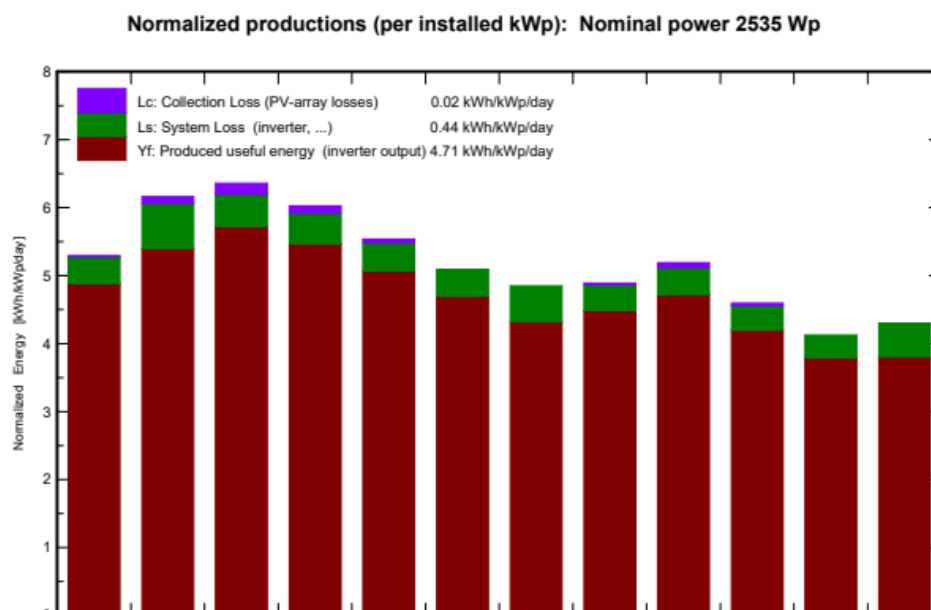
Figure 19: Normalized Energy production

Daily System energy output
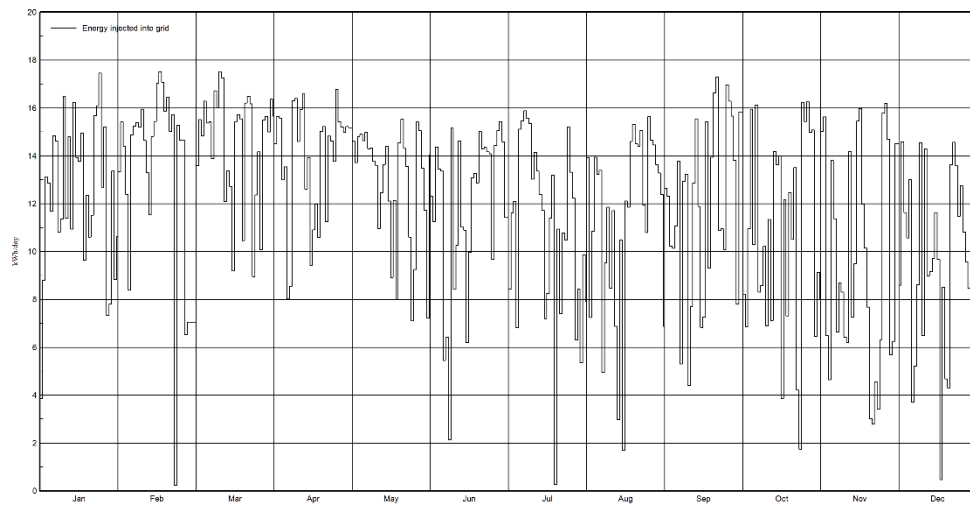
Figure 20: Daily system energy output

The beginning of summer from Feb to May produce the most power compared to other seasons and the collection losses are most in seasons of heavy winds and precipitation. June and july are the months with minimal collection losses because of tranquil climatic conditions in those months.

System Ouput Power Distribution

The power distribution shows the power that is distributed to the power grid and how much power is injected
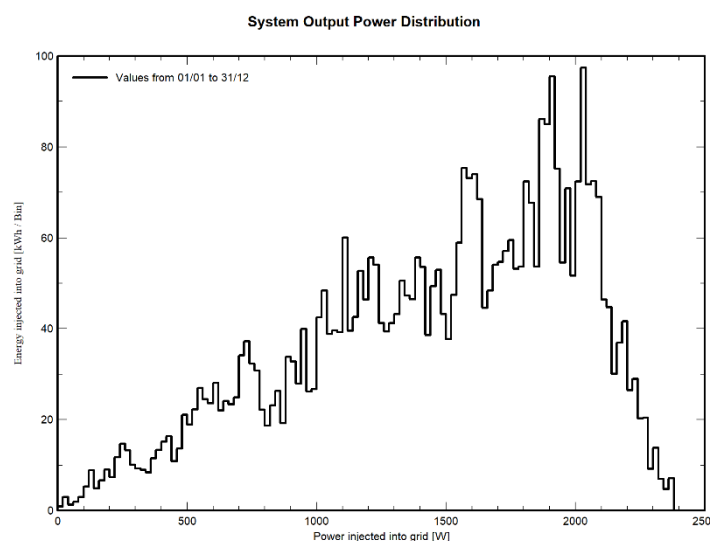
Figure 21: Power Distribution

Energy produced each year with varying tilt angles.

From Figure 20 with further research into the optimum tilt angle for the specified location has given more input into the energy produced for each angle .
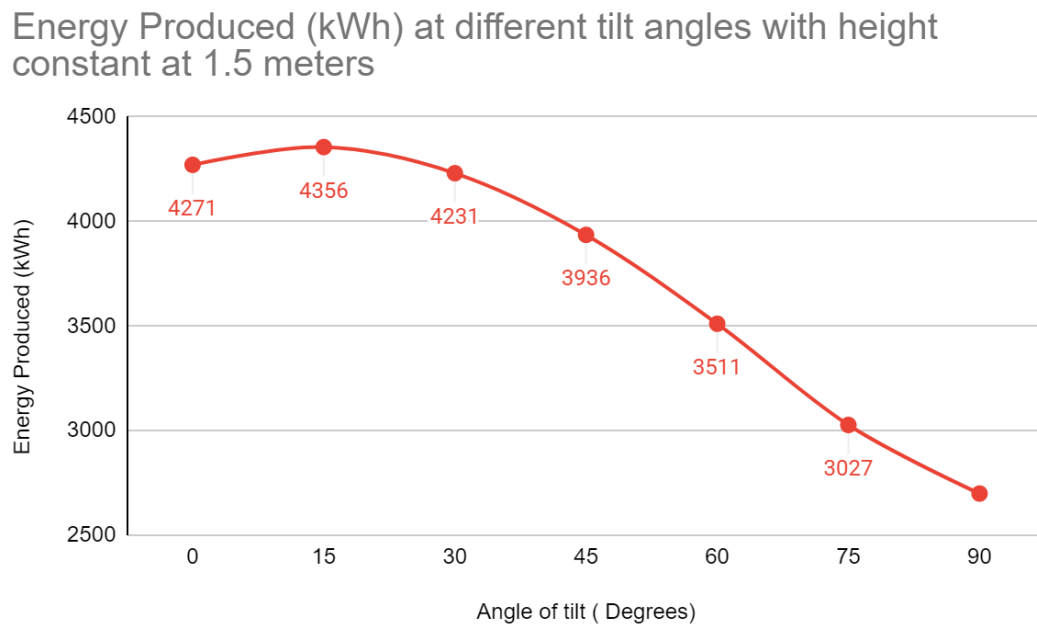
Figure 22: Energy produced at different tilt angles

Tilt angle and orientation are important parameters to be taken into account while modelling a solar panels as they play ahuge role in collection of irradiance from the sun and also in accumlating the reflected rays from the ground. The graph given shows the variation of energy produced for various angles of tilt. The energy produced reaches the peak at 15° and then decreases thereafter as the angle increases . Thus, 15° was considered to be the optimum angle for our site.

Energy Produced each year with varying heights.

Referring Figure 21, At 15°, which was found to be the optimum angle, the variation in energy produced for different heights was studied. The increase in height does have an effect on the energy produced by the solar grid system but only to an extent. The above given graph shows the increase in energy produced by the solar panels with increase in height of 0.5m increments.

Energy Produced (kWh) at different heights with constant tilt angle at 15°

Figure 23: Energy produced at different heights

There was a steep increase in energy produced when the height was increased from 1m to 1.5m and thereafter the steep started to flatten out when the height reached 2.5m. The increase in energy was in about 10 units from p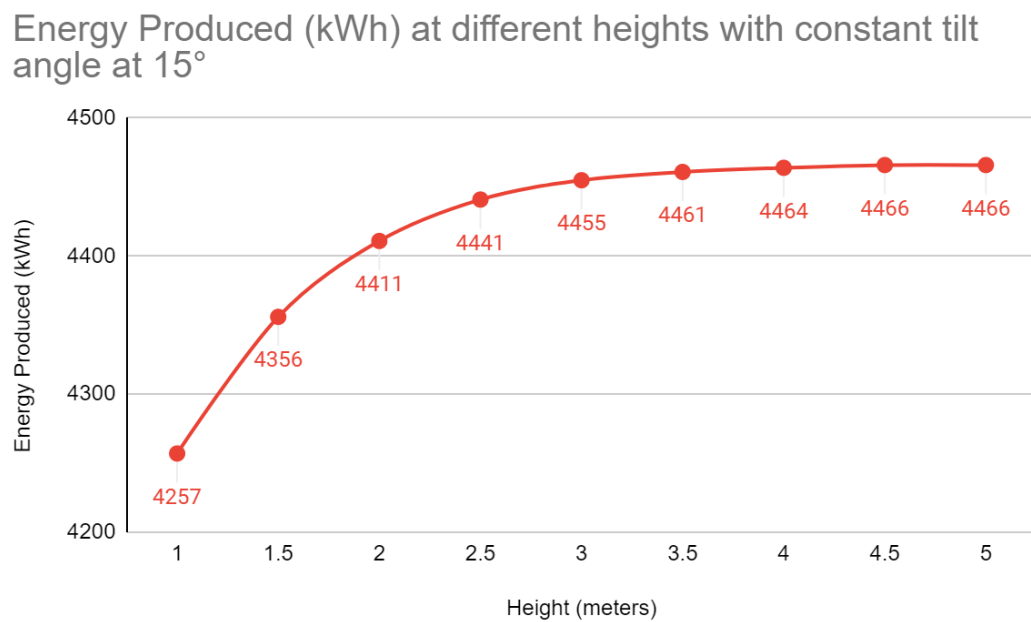reviously recorded increase of nearly 100 units. After further increase in height, at 5m, the increase in energy was negligible.

4.2 Simulation using PVsyst (After Consumption)

The energy consumptions are monitored to be 30 kWh/day or 10950 kWh/year.

4.2.1 System Parameters

Project summary

Geographical Site	Situation		Project settings	
Geographical Site	**Situation**		**Project settings**	
Kattankulathur	Latitude	12.82 °N	Albedo	0.20
India	Longitude	80.04 °E		
	Altitude	43 m		
	Time zone	UTC+5.5		
Meteo data				
Kattankulathur				
Meteonorm 8.0 (1996-2015) - Synthetic				

System summary

Grid-Connected System — Unlimited sheds

PV Field Orientation		Near Shadings		User's needs	
Sheds		Mutual shadings of sheds		Fixed constant load	
tilt	15 °	Electrical effect		1250 W	
azimuth	0 °			Global	
				10.95 MWh/Year	

System information

PV Array		Inverters		Battery pack	
Nb. of modules	13 units	Nb. of units	1 Unit	Storage strategy: Self-consumption	
Pnom total	2535 Wp	Pnom total	2500 W	Nb. of units	1 Unit
		Pnom ratio	1.014	Voltage	720 V
				Capacity	222 Ah

Results summary

Produced Energy	4356 kWh/year	Specific production	1718 kWh/kWp/year	Perf. Ratio PR	90.10 %
				Solar Fraction SF	39.37 %

Figure 24: System parameters

For after consumption of the energy produced the by the grid based solar system, the same parameters are taken along with the same geographical site but only with the inclusion of a battery pack for the storage of the energy produced.

4.2.2 Storage Strategy

The storage strategy follows a very simple system of 'Energy consumed when provided and used when required'.

Storage

Kind	Self-consumption		
Charging strategy		**Discharging strategy**	
When excess solar power is available		As soon as power is needed	

4.2.3 Loss Diagram

The loss diagrams are more or less same when compared to that of before consumption. Figure 21. that shows loss due to irradiance of the sun has no changes whereas Figure 22.
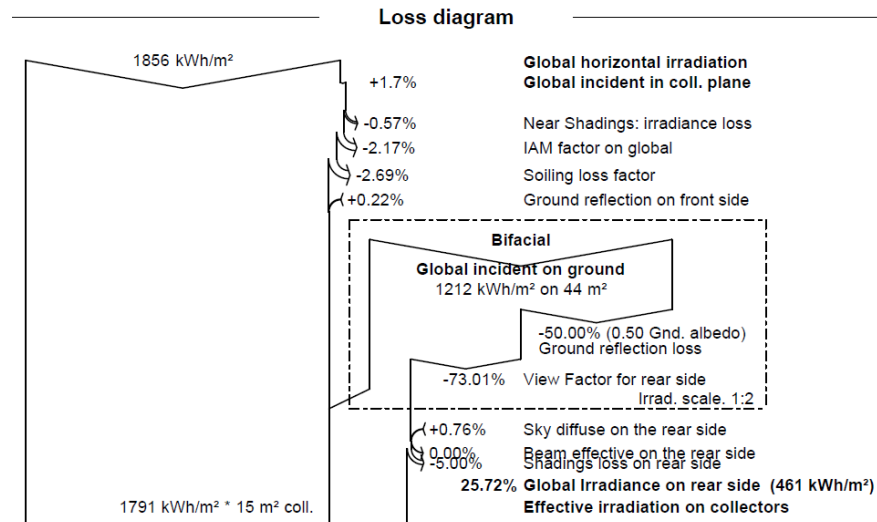

Figure 25: Loss diagram for sun irradiance (after consumption)
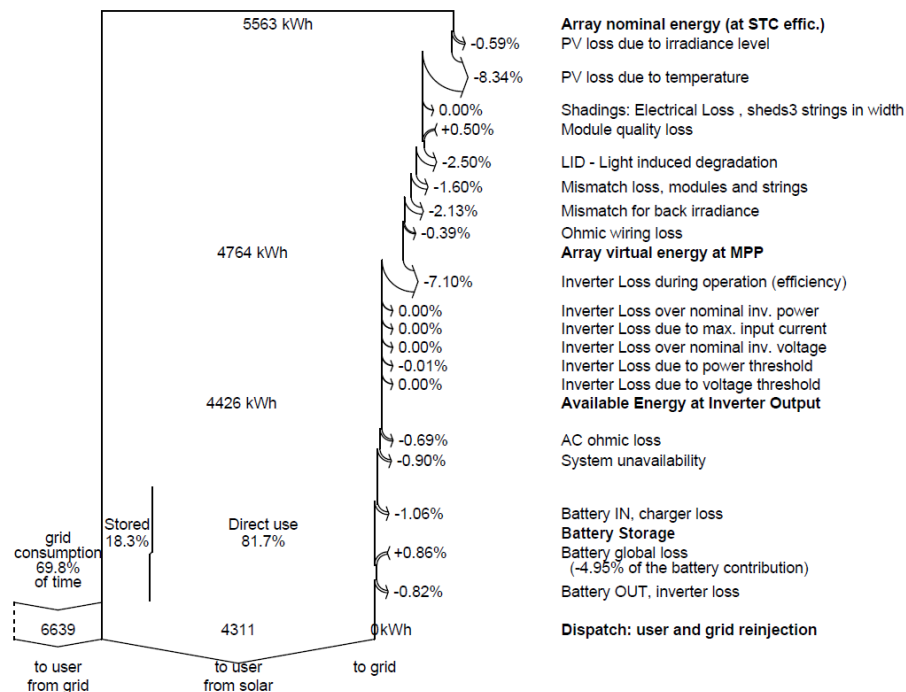

Figure 26: Loss diagram for panel output (after consumption)

Which shows the loss of the panel output incurs more loss due to the effect of the battery installed to store the energy produced. After considering the global loss of the battery we can see that the energy produced by the grid to the user decreases from 4356 kWh to 4311 kWh.

4.2.4 Simulation Result and Graphs

GlobHor is the global horizontal energy that is avaiable to the system at that particular month of the year. DiffHor is the diffused horizontal energy which is available to the system at the same period of time. T_Amb is the temperature of the system surroundings.
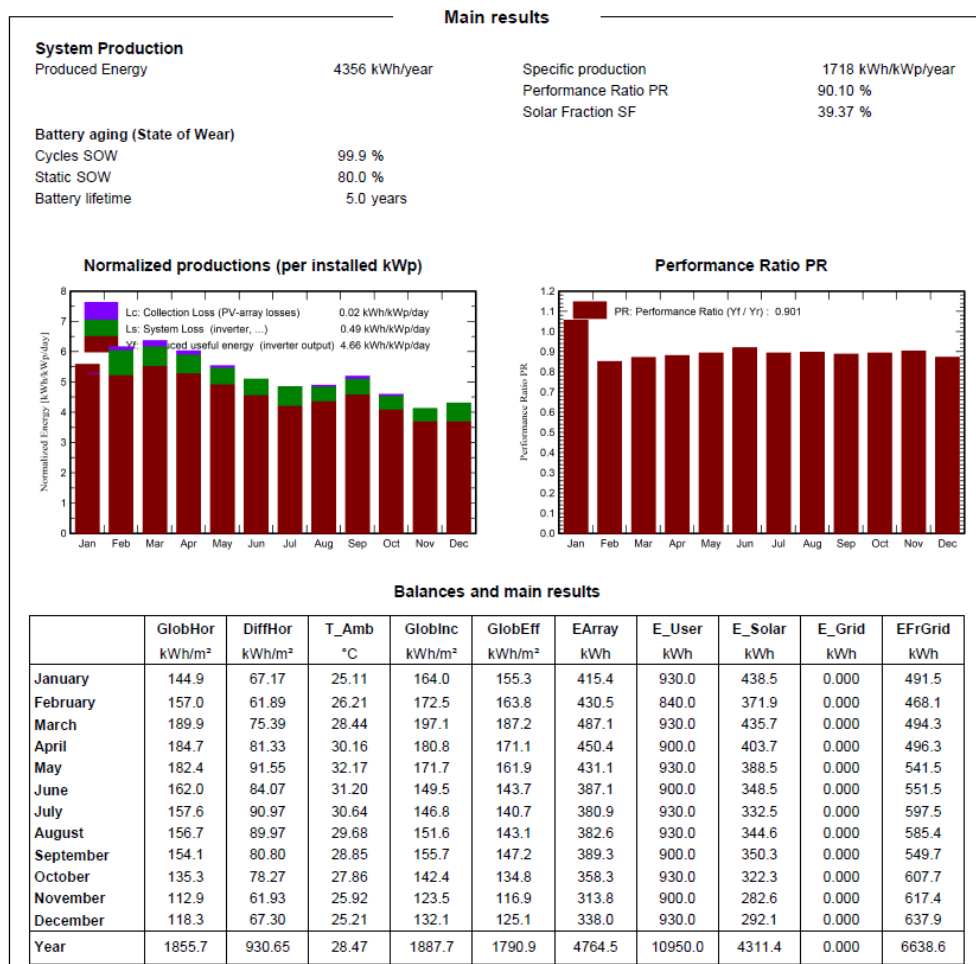

Main results

System Production

Produced Energy	4356 kWh/year	Specific production	1718 kWh/kWp/year
Performance Ratio PR			90.10 %
Solar Fraction SF			39.37 %

Battery aging (State of Wear)

Cycles SOW	99.9 %
Static SOW	80.0 %
Battery lifetime	5.0 years

Balances and main results

	GlobHor	DiffHor	T_Amb	GlobInc	GlobEff	EArray	E_User	E_Solar	E_Grid	EFrGrid
	kWh/m²	kWh/m²	°C	kWh/m²	kWh/m²	kWh	kWh	kWh	kWh	kWh
January	144.9	67.17	25.11	164.0	155.3	415.4	930.0	438.5	0.000	491.5
February	157.0	61.89	26.21	172.5	163.8	430.5	840.0	371.9	0.000	468.1
March	189.9	75.39	28.44	197.1	187.2	487.1	930.0	435.7	0.000	494.3
April	184.7	81.33	30.16	180.8	171.1	450.4	900.0	403.7	0.000	496.3
May	182.4	91.55	32.17	171.7	161.9	431.1	930.0	388.5	0.000	541.5
June	162.0	84.07	31.20	149.5	143.7	387.1	900.0	348.5	0.000	551.5
July	157.6	90.97	30.64	146.8	140.7	380.9	930.0	332.5	0.000	597.5
August	156.7	89.97	29.68	151.6	143.1	382.6	930.0	344.6	0.000	585.4
September	154.1	80.80	28.85	155.7	147.2	389.3	900.0	350.3	0.000	549.7
October	135.3	78.27	27.86	142.4	134.8	358.3	930.0	322.3	0.000	607.7
November	112.9	61.93	25.92	123.5	116.9	313.8	900.0	282.6	0.000	617.4
December	118.3	67.30	25.21	132.1	125.1	338.0	930.0	292.1	0.000	637.9
Year	1855.7	930.65	28.47	1887.7	1790.9	4764.5	10950.0	4311.4	0.000	6638.6

Figure 27: Main results (after consumption)

EArray again is the amount of energy that the array of panels are able to produce througought the year. E_User is the amount of energy used by the user, here we have an usuage of 30kWh/day. Consdering the factors the usage changes. As the energy produced is self-

sufficient, no excess energy is sent to the grid. EFrGrid is the amount energy that is received from the grid as during the night, the system does not produce any energy. The battery used is small as well, so the during the night the current is received from the grid.

4.2.5 Energy from the grid

The energy that is received from the grid during off sunshine hours are as shown. Till from sunrise, that is 6AM there is drop in energy that is taken from the grid. By 9AM the system is self-sufficient to run the appliances and household needs by itself without the help of the grid energy.
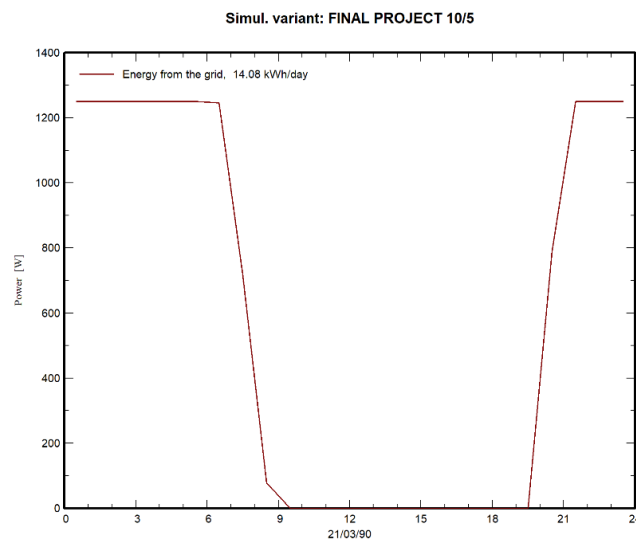

Figure 28: Energy from grid

Up until 5PM where the sun is no longer available, the system makes use of the small battery that it had stored during excess energy production. From Table 6 we can see that the off-sunshine hours start at 6PM. Meaning till 7:30PM the system won't be needing the energy from the grid. After 7:30PM again the energy is received from the grid to run the appliances that were forementioned. This can be further decreased by increasing the size of the battery if required.

By installing the panel, the system was self sufficient to run the household energy requirement during the day time. And further proves that this system is self- sufficient during the sunshine hours.

CHAPTER: 5 CONCLUSIONS

5.1 Information Inferred from the Test and Simulation

We were able to learn that the bifacial panel is a technology that can be improved vastly on main different factors starting from improving the setup to its surroundings to improve the overall efficiency of the panel or grid output.

From the tests that were performed on the simulation, we were able to find the optimal angle for the panel, which was found to be 15°. The tilt angle of 15° gives the maximum output because this angle is the closest to the latitude of the location which is 13.0827° N.

The optimal height was found out to be somewhere from 1.5 meters to 2.5 meters (depends on the location it is being setup). The increase in output in energy from 1 meter to 1.5 meter was quite noticeable in both mathematical as well as the simulation. Whereas the increase from 1.5 meters or from 2 meters to 2.5 meters was not large but it was still significant if seen for year around production. But any increase in height of above 2.5 meters does not produce any much increase in output level that will justify its cost for the structure.

It also has to be noted that with increase in height, wind force experienced by the panel increases as it moves away from the ground. The support structure would need more failproof design and stronger mounts. This increases the cost of the setup and will not justify the performance to cost ratio.

For the best result and best performance to cost ratio, from the analysis performed we can conclude that the best angle for bifacial photovoltaic system will be 15° and at a height of 1.5 meters.

CHAPTER 6: FUTURE ENHANCEMENTS

6.1 Future of Bifacial Industry

The 'International Technology Roadmap for Photovoltaics' predict that the bifacial systems will have much more market share by the year of 2030 with a ratio of 70% bifacial to 30% monoracial.
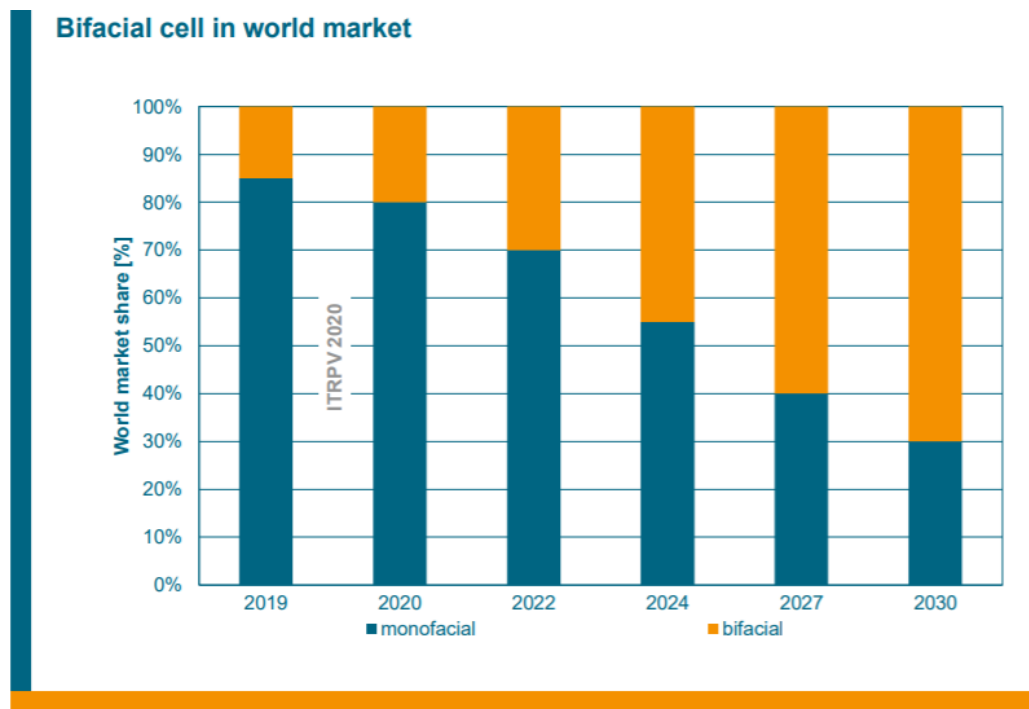

Figure 29: Market share of bifacial cell

6.2 Future of the Project

As mentioned earlier in conclusion, the scope for improvement in this field is vast and can be done to the system in itself or to the surroundings around the system to tweak its output performance. There are several factors that can be tweaked for further enhancement. The factors depend on other external factors like temperature, albedo and so on. This is only conditional to certain scenarios. But as a whole, these energy gains should be balanced with increased installation cost to make sure there is economic viability and still gives the best results from the setup. The major areas that can be further worked on are stated below.

6.2.1 Different Surfaces

One of the ways is to increase the albedo, this can be done using different type of materials. Aluminum and white paint gains more reflectivity and increases the albedo.

6.2.2 Using Reflectors

Using reflectors like mirror or aluminum which can efficiently reflect the light straight at the module will increase the output. Materials that can be used are white paint, paper, silver coated mirror, PTFE.

6.2.3 Decreasing the Shading on Modules

Shading and self-shading can cause loss in output, this can be avoided by enough space between panels and any obstacles around it.

6.2.3 Taking care of Soiling

Around the year, soiling will occur. During the dry season, due to wind, dust build up will occur. Modules will need a periodic maintenance and cleaning to keep their output constant throughout the year.

CHAPTER 7: REFERENCES

1. Min Hsian Saw, Yong Sheng Khoo, Jai Prakash Singh, and Yan Wang. "Enhancing optical performance of bifacial PV modules", *Energy Procedia* 124 (2017): 484-494.

2. Wenbo Gu, Senji Li, Xing Liu, Zhenwu Chen, Xiaochun Zhang, and Tao Ma. "Experimental investigation of the bifacial photovoltaic module under real conditions", *Renewable Energy* (2020).

3. Xingshu Sun, Mohammad Ryyan Khan, Chris Deline, and Muhammad Ashraful Alam. "Optimization and performance of bifacial solar modules: A global perspective", *Applied energy* 212 (2018): 1601-1610.

4. Stanley Wang, Oscar Wilkie, Jenny Lam, Rob Steeman, Wilson Zhang, Kah Sing Khoo, Sim Chun Siong, and Hannes Rostan. "Bifacial photovoltaic systems energy yield modelling", *Energy Procedia* 77 (2015): 428-433.

5. Ismail Shoukry, Joris Libal, Radovan Kopecek, Eckard Wefringhaus, and Jürgen Werner. "Modelling of bifacial gain for stand-alone and in-field installed bifacial PV modules", *Energy Procedia* 92 (2016): 600-608.

6. Enric Grau Luque, Fernando Antonanzas-Torres, and Rodrigo Escobar. "Effect of soiling in bifacial PV modules and cleaning schedule optimization", *Energy Conversion and Management* 174 (2018): 615-625.

7. Judith Frank, Marc Rüdiger, Stefan Fischer, Jan Christoph Goldschmidt, and Martin Hermle. "Optical simulation of bifacial solar cells", *Energy Procedia* 27 (2012): 300-305.

8. Raina Gautam, and Sunanda Sinha. "A simulation study to evaluate and compare monofacial Vs bifacial PERC PV cells and the effect of albedo on bifacial performance." *Materials Today: Proceedings* (2020).

9. Katsaounis, Th, K. Kotsovos, Issam Gereige, A. Basaheeh, M. Abdullah, A. Khayat, E. Al-Habshi, A. Al-Saggaf, and A. E. Tzavaras. "Performance assessment of bifacial c-Si PV modules through device simulations and outdoor measurements." *Renewable Energy* 143 (2019): 1285-1298.

10. Nussbaumer, Hartmut, Markus Klenk, Marco Morf, and Nicolas Keller. "Energy yield prediction of a bifacial PV system with a miniaturized test array." *Solar Energy* 179 (2019): 316-325.

11. Patel, M. Tahir, Ramachandran A. Vijayan, Reza Asadpour, M. Varadharajaperumal, M. Ryyan Khan, and Muhammad A. Alam. "Temperature-dependent energy gain of bifacial PV farms: A global perspective." *Applied Energy* 276 (2020): 115405

12. Baumann, Thomas, Hartmut Nussbaumer, Markus Klenk, Andreas Dreisiebner, Fabian Carigiet, and Franz Baumgartner. "Photovoltaic systems with vertically mounted bifacial PV modules in combination with green roofs." *Solar Energy* 190 (2019): 139-146.

13. Zhu, Qiangzhong, Chen Zhu, Songmin Liu, Chanjun Shen, Wei Zhao, Zhenbo Chen, Ling Chen et al. "A model to evaluate the effect of shading objects on the energy yield gain of bifacial modules." *Solar Energy* 179 (2019): 24-29.

14. Chudinzow, Dimitrij, Jannik Haas, Gustavo Díaz-Ferrán, Simón Moreno-Leiva, and Ludger Eltrop. "Simulating the energy yield of a bifacial photovoltaic power plant." *Solar Energy* 183 (2019): 812-822.

15. Stanley Wang, Oscar Wilkie, Jenny Lam, Rob Steeman, Wilson Zhang, Kah Sing, Khoo, Sim Chun Siong, Hannes Rostan. "Bifacial photovoltaic systems energy yield modelling", *Energy Procedia* 77 (2015) 428-433.

16. Gu, Wenbo, Tao Ma, Meng Li, Lu Shen, and Yijie Zhang. "A coupled optical-electrical-thermal model of the bifacial photovoltaic module." *Applied Energy* 258 (2020): 114075.

17. Ahmer A.B. Baloch, Said Hammat, Benjamin Figgis, Fahhad H. Alharbi, Nouar Tabet, "In-field characterization of key performance parameters for bifacial photovoltaic installation in a desert climate", *Renewable Energy*, 159 (2020) 50-63.

18. Wenhao Chena, Renzhong Liub, Qingguo Zenga, Lang Zhoua, "Low cost multicrystalline bifacial PERC solar cells – Fabrication and thermal improvement", *Solar Energy*, 184 (2019) 508-514.

19. Ryyan Khan, M., Amir Hanna, Xingshu Sun, and Muhammad A. Alam. "Vertical bifacial solar farms: Physics, design, and global optimization." *Applied energy* 206 (2017): 240-248.0

20. Kuo, Chung-Feng Jeffrey, Pei-Chung Yang, Mega Lazuardi Umar, and Wei-Lun Lan. "A bifacial photovoltaic thermal system design with parameter optimization and performance beneficial validation." *Applied Energy* 247 (2019): 335-349.

21. Lopez-Garcia, Juan, Alberto Casado, and Tony Sample. "Electrical performance of bifacial silicon PV modules under different indoor mounting configurations affecting the rear reflected irradiance." *Solar Energy* 177 (2019): 471-482.

22. Guerrero-Lemus, R., R. Vega, Taehyeon Kim, Amy Kimm, and L. E. Shephard. "Bifacial solar photovoltaics–A technology review." *Renewable and sustainable energy* (2016): 1533-1549.

23. Ledesma, J. R., R. H. Almeida, F. Martinez-Moreno, C. Rossa, J. Martín-Rueda, L. Narvarte, and E. Lorenzo. "A simulation model of the irradiation and energy yield of large bifacial photovoltaic plants." *Solar Energy* 206 (2020): 522-538.

24. Razongles, Guillaume, Lionel Sicot, Maryline Joanny, Eric Gerritsen, Paul Lefillastre, Silke Schroder, and Philippe Lay. "Bifacial photovoltaic modules: measurement challenges." *Energy Procedia* 92 (2016): 188-198

25. Gu, Wenbo, Tao Ma, Salman Ahmed, Yijie Zhang, and Jinqing Peng. "A comprehensive review and outlook of bifacial photovoltaic (bPV) technology." *Energy Conversion and Management* 223 (2020): 113283.

26. Janssen, Gaby JM, Bas B. Van Aken, Anna J. Carr, and Agnes A. Mewe. "Outdoor performance of bifacial modules by measurements and modelling." *Energy Procedia* 77 (2015): 364-373.

27. Yusufoglu, Ufuk Alper, Tae Hun Lee, Tobias Markus Pletzer, Andreas Halm, Lejo Joseph Koduvelikulathu, Corrado Comparotto, Radovan Kopecek, and Heinrich Kurz. "Simulation of energy production by bifacial modules with revision of ground reflection." *Energy Procedia* 55 (2014): 389-395.

28. Yusufoglu, Ufuk Alper, Tae Hun Lee, Tobias Markus Pletzer, Andreas Halm, Lejo Joseph Koduvelikulathu, Corrado Comparotto, Radovan Kopecek, and Heinrich Kurz. "Simulation of energy production by bifacial modules with revision of ground reflection." *Energy Procedia* 55 (2014): 389-395.

29. Zhang, Zhen, Minyan Wu, Yue Lu, Chuanjia Xu, Lei Wang, Yunfei Hu, and Fei Zhang. "The mathematical and experimental analysis on the steady-state operating temperature of bifacial photovoltaic modules." *Renewable Energy* 155 (2020): 658-668.

30. Appelbaum, J. J. R. E. "Bifacial photovoltaic panels field." *Renewable Energy* 85 (2016): 338-343.

31. Yin, H. P., Y. F. Zhou, S. L. Sun, W. S. Tang, W. Shan, X. M. Huang, and X. D. Shen. "Optical enhanced effects on the electrical performance and energy yield of bifacial PV modules." *Solar Energy* 217 (2021): 245-252.

32. Lorenzo, Eduardo. "On the historical origins of bifacial PV modelling." *Solar Energy* 218 (2021): 587-595.

<table>
<tr><td colspan="3" align="center">**Format I**
SRM INSTITUTE OF SCIENCE AND TECHNOLOGY
(Deemed to be University u/s 3 of UGC Act, 1956)</td></tr>
</table>

Format I
SRM INSTITUTE OF SCIENCE AND TECHNOLOGY
(Deemed to be University u/s 3 of UGC Act, 1956)

Office of Controller of Examinations

REPORT FOR PLAGIARISM CHECK ON THE PROJECT REPORT FOR UG/PG PROGRAMMES
(To be attached in the Project Report)

1	Name of the Candidate(s)	**A. RAHUL ARAVIND**
		PRASANTH CHOWDARY . Y
2	Address of the Candidate	Department of Mechanical Engineering, SRM Institute of Science and Technology, SRM Nagar, Kattankulathur 603203. Mobile Number of Candidate 1: 8939119379 Mobile Number of Candidate 2: 8825953241
3	Registration Number of the Candidate(s)	RA1711002010024
		RA1711002010049
4	Date of Birth of the Candidate(s)	05 / 03 / 1999
		04 / 09 / 1999
5	Department	Mechanical Engineering
6	Faculty	Engineering and Technology
7	Title of the Project	Modelling and simulation of Bifacial solar PV systems.
8	Name and address of the Supervisor	**Mr. Joji Johnson** Department of Mechanical Engineering, SRM Institute of Science and Technology, SRM Nagar, Kattankulathur 603203. **E-mail: jojij@srmist.edu.in** **Mobile: +91 9884214230**
9	Name and address of the Co-Supervisor (if any)	**Not Applicable**
10	Software Used	TURNITIN
11	Date of Verification	21 MAY 2021

12	Plagiarism Details: (to attach the final report from Turnitin)			
Chapter	Title of the Chapter	Percentage of similarity index (including self citation)	Percentage of similarity index (Excluding self citation)	% of plagiarism after excluding Quotes, Bibliography, etc.,
1	Introduction	0	0	0
2	Literature Review	<1	<1	<1
3	System Analysis	<1	<1	<1
4	Simulation	<1	<1	<1
5	Conclusion	0	0	0
6	Future Enhancement	0	0	0
7	References	0	0	0
8				
Appendices		1	1	1
Total Plagiarism percentage		2		

I / We declare that the above information have been verified and found true to the best of my / our knowledge.

PRASANTH CHOWDARY.Y

A.RAHUL ARAVIND

Signature of the Candidate(s)

Vengatraman S

Name and Signature of the staff performed Plagiarism Check with date

Name and Signature of the Guide	**Name and Signature of the Head of the Department**

T24

1   "ELECTRIC POWER AND ENERGY MEASUREMENT", Handbook of Measurement in Science and Engineering, 2016.
    Publication   **1**%

2   www.mdpi.com
    Internet Source   <**1**%

3   doi.org
    Internet Source   <**1**%

4   Eric Blades, Parthiv N. Shah, Michael Nucci, Scott Miskovish. "Demonstration of Multiphysics Analysis Tools on Representative Hypersonic Vehicle Structures", 54th AIAA/ASME/ASCE/AHS/ASC Structures, Structural Dynamics, and Materials Conference, 2013
    Publication   <**1**%

5   Dimitrij Chudinzow, Jannik Haas, Gustavo Díaz-Ferrán, Simón Moreno-Leiva, Ludger Eltrop. "Simulating the energy yield of a bifacial photovoltaic power plant", Solar Energy, 2019   <**1**%

Exclude quotes   On
Exclude bibliography On

Exclude matches   < 10 words